How to cite: *Angew. Chem. Int. Ed.* **2022,** *61,* e202117394
International Edition: doi.org/10.1002/anie.202117394
German Edition: doi.org/10.1002/ange.202117394

CH Activation

Supported Lanthanum Borohydride Catalyzes CH Borylation Inside Zeolite Micropores

Yuting Li, Uddhav Kanbur, Jinlei Cui, Guocang Wang, Takeshi Kobayashi, Aaron D. Sadow, and Long Qi**

Abstract: The zeolite-supported lanthanide $La(BH_4)_x$-HY_{30} catalyzes C–H borylation of benzene with pinacolborane (HBpin), providing a complementary approach to precious, late transition metal-catalyzed borylations. The reactive catalytic species are generated from La grafted at the Brønsted acid sites (BAS) in micropores of the zeolite, whereas silanoate- and aluminoate-grafted sites are inactive under the reaction conditions. During typical catalytic borylations, conversion to phenyl pinacolborane (PhBpin) is zero-order in HBpin concentration. A turnover number (TON) of 167 is accessed by capping external silanols, selectively grafting at BAS sites, and adding HBpin slowly to the reaction.

Hydrocarbon C–H borylation with pinacol diborane (B_2pin_2), efficiently catalyzed by Group 9 organometallics,[1] is a single-step functionalization that provides versatile organoboranes.[1a–c,2] Catalysts that access new mechanisms or distinct selectivity for C–H borylation, utilize earth-abundant metal centers such as lanthanum (an overproduced co-product of technologically essential rare earth elements), or use the pinacolborane (HBpin) reagent could complement late metal catalysts that currently dominate this transformation. In particular, catalysts employing d^0 or d^0f^n centers are appealing for new C–H borylations, given well-established C–H bond activations mediated[3] or catalyzed[4] via elementary σ-bond metathesis reactions.[5] Despite early promise,[6] the sole example of rare earth-catalyzed C–H borylation involves *ortho*-directed derivatization of aromatic ethers catalyzed by 5–10 mol % $(C_5Me_4H)_2LnR$ (Ln = Y, Lu).[7] Reactants and ancillary ligands' steric properties, coordination of the aryl ether, and catalyst deactivation by ring-opening of HBpin are important factors in that catalysis.

Oxide-supported, confined organolanthanide compounds could potentially tolerate elevated reaction temperatures and access low-coordinate metal centers needed for C–H bond activations. Because [Ln]H·HBpin adducts are proposed to directly react with carbonyls or epoxides during catalytic hydroboration reactions or act as masked hydrides,[8] we hypothesized that related species from lanthanide borohydrides could mediate borylation of hydrocarbons. Cationic molecular and surface-supported lanthanide borohydride complexes also have shown promise in ring-opening and addition polymerization of esters.[9,10] In addition, late metal complexes supported on metal–organic frameworks (MOFs)[11] or periodic mesoporous organosilicas (PMOs)[12] have provided efficient catalysts for C–H borylation, often showing the benefits of site isolation.[11a–e] Metal centers supported on zeolites are well known to catalyze other conversions of hydrocarbons with size and shape selectivity.[13] Here, we identify lanthanide borohydride species grafted at the bridging Si–OH–Al Brønsted acid sites (BAS) in zeolite micropores as catalysts for C–H borylation and describe strategies for increasing turnover number (TON), guided by solid-state nuclear magnetic resonance (SS NMR), diffuse reflectance infrared Fourier-transform spectroscopy (DRIFTS), and kinetic analysis.

First, $La(BH_4)_3(THF)_3$ grafted onto inorganic supports, including SiO_2, γ-Al_2O_3, SiO_2/Al_2O_3, or the microporous faujasite zeolite HY_{30} (Si/Al = 30) were compared as potential catalysts for C–H borylation of benzene. The latter two supports contain heteroatomic bridging hydroxy as BAS, which are mostly isolated in the highly siliceous HY_{30} (< one per supercage; Figure S1). All supports were treated at 500 °C under dynamic vacuum, and then $La(BH_4)_3(THF)_3$ was grafted in toluene for 24 h at room temperature (see Supporting Information for details; Figures S2, S3). The isolated materials (Table 1) were characterized by elemental analysis to determine lanthanum loading, as well as by DRIFTS and SS NMR spectroscopy to identify BH-containing groups, organic species, Brønsted acids, and silanols on the support before and after grafting (see below).

The HBpin starting material was the only borane species observed in attempted CH borylations of benzene using ≈0.2 mol % of either unsupported $La(BH_4)_3(THF)_3$, $La(BH_4)_x(THF)_n$-SiO_2, or $La(BH_4)_x(THF)_n$-Al_2O_3, as precatalysts, and phenyl pinacolborane (PhBpin) was not detected in the mixture. We infer that neither $(\equiv SiO)_{3-x}La(BH_4)_x$-

[*] Dr. Y. Li, Dr. U. Kanbur, Dr. J. Cui, Dr. G. Wang, Dr. T. Kobayashi, Prof. A. D. Sadow, Dr. L. Qi
U.S. DOE Ames Laboratory, Iowa State University, Ames, IA 50011 (USA)
E-mail: sadow@iastate.edu
lqi@iastate.edu
Dr. U. Kanbur, Prof. A. D. Sadow
Department of Chemistry, Iowa State University
Ames, IA 50011 (USA)

Table 1: C–H borylation of benzene catalyzed by lanthanum borohydride complexes.[a]

Catalyst	La [mmol g^{-1}][b]	La [mo %][c]	Conversion [%]	Yield [%]	Turnovers	Selectivity [%]
$La(BH_4)_3(THF)_3$	n/a	0.18	≈0	0	n/a	n/a
$La(BH_4)_x(THF)_n$-SiO_2	0.14	0.36	≈0	0	n/a	n/a
$La(BH_4)_x(THF)_n$-Al_2O_3[d]	0.02	0.18	≈0	0	n/a	n/a
$La(BH_4)_x(THF)_n$-SiO_2/Al_2O_3	0.09	0.22	100	1.3	6	1.1
$La(BH_4)_x(THF)_n$-HY_{30}	0.07	0.18	100	1.8	10	1.8
$La(BH_4)_2(THF)_{2.5}$-TPS-HY_{30}	0.05	0.12	95	7.4	62	7.8

[a] Reaction conditions: 50 mg catalyst, 1 mL benzene and 0.3 mL HBpin (0.002 mol) at 120 °C for 12 h. [b] Loading of La [mmol g^{-1}] in catalytic materials measured by ICP-OES. [c] Molar percentage [mol %] of La to HBpin. [d] 150 mg.

$(THF)_n$-type sites grafted by reaction with surface OH in silica or alumina nor cationic $[La(BH_4)_x(THF)_n]^+$ resulting from activation at Lewis acid sites (LAS) in γ-Al_2O_3 are catalytically active for C–H borylation of benzene under these conditions. In contrast, HBpin was completely consumed in neat benzene and in the presence of $La(BH_4)_x$-$(THF)_n$-SiO_2/Al_2O_3 or $La(BH_4)_x(THF)_n$-HY_{30} as precatalysts, giving 1.1 % and 1.8 % yield of PhBpin, which corresponds to turnovers of 6 and 10 (moles PhBpin/mols La). Although the initial precatalyst formulations and reaction conditions give low yields and poor selectivity for PhBpin, the experiments importantly provided new insight that $La(BH_4)_x$ species bonded at BAS, the functionality that is common to SiO_2/Al_2O_3 and zeolite HY_{30} but not SiO_2 or γ-Al_2O_3, are catalytically active for CH borylation of benzene.

We then identified the surface species on the bare La-free supports capable of decomposing HBpin, by examining reactions of HBpin with the calcined oxides, to develop strategies for increasing benzene borylation yields by limiting the undesired pathway. SiO_2 or γ-Al_2O_3 gave constant HBpin concentration after heating with HBpin and benzene for 2 h at 120 °C (Table S1), ruling out silanol, aluminol, and LAS sites as catalysts for HBpin decomposition. In contrast, HBpin was quantitatively consumed within 2 h in the presence of BAS-containing HY_{30} and SiO_2/Al_2O_3, while PhBpin was not detected in these experiments. Considering these observations and the hypothesis that lanthanum species grafted on BAS are the active sites, strategies to improve catalytic performance could involve selective placement of lanthanum borohydrides at all bridging Si–OH–Al moieties. DRIFTS analysis (Figure S4), however, showed that nearly all silanols in the SiO_2/Al_2O_3 and HY_{30} had been consumed during grafting, giving a high proportion of inactive La species.

We designed an approach for grafting La selectively at the BAS in HY_{30} to improve the performance of this catalyst. The Si–OH–Al BAS are primarily located in microporous cages (Figure S1) while silanols are mainly on the external surface after thermal treatment at 500 °C.[14] This spatial segregation suggested that silanol capping with Ph_3SiCl (TPSCl) could block unwanted grafting of La-$(BH_4)_3(THF)_3$ on the external surface. TPSCl is too large (≈10 Å diameter) to enter the 7.35 Å micropores and react with BAS in HY_{30}. $La(BH_4)_x(THF)_n$-HY_{30} also provided slightly higher turnovers, yield, and selectivity for PhBpin than the SiO_2/Al_2O_3-grafted catalyst, which cannot be selectively capped. In addition, selective grafting of La-$(BH_4)_3(THF)_3$ on the BAS adjacent to crystallographically equivalent Al-based T4 positions in HY_{30} could provide a single-site catalyst with structurally uniform sites.

Silanol capping with TPSCl affords the silylated zeolite TPS-HY_{30} on a 2 g scale (see Supporting Information). The normalized intensity of the ν_{SiOH} signal at 3746 cm^{-1} in the DRIFTS of TPS-HY_{30} was decreased by 54 % compared to that of the HY_{30} starting material (Figure 1),[15] while BAS-assigned signals at 3630 and 3566 cm^{-1} were constant in the two samples.[16] In addition, the similar pattern of peaks from ca. 3100–2850 cm^{-1} associated with ν_{CH} in TPSCl (Figure S4) and in the modified zeolite indicate that organosilyl groups were grafted on HY_{30}. These grafted Ph_3*Si*-OSi surface species were unambiguously assigned to a signal at −20 ppm in the $^{29}Si\{^1H\}$ cross-polarization magic angle spinning (CPMAS) SS NMR spectrum of TPS-HY_{30} (Figure S5).[17] Finally, TPS-HY_{30} and HY_{30} mediated HBpin decomposition in comparable times (2 h), reinforcing the notion that BAS are similarly available inside the pores of TPS-HY_{30} and HY_{30}, as well as that capping primarily sequesters the external silanols.

Reaction of $La(BH_4)_3(THF)_3$ and TPS-HY_{30} affords $La(BH_4)_2(THF)_{2.5}$-TPS-HY_{30} (composition established below). The 0.75 La wt % in the TPS-capped zeolite is expectedly lower than 1.0 La wt % in unprotected $La(BH_4)_x$-

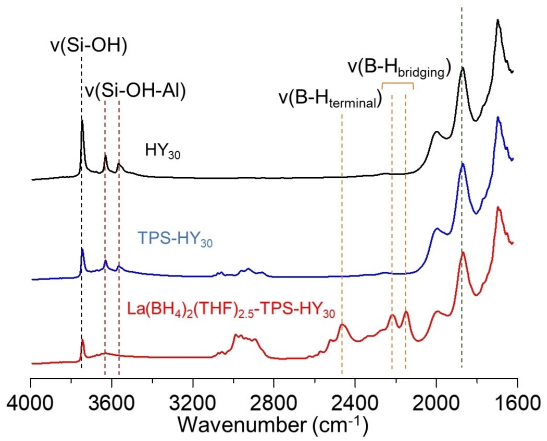

Figure 1. DRIFTS spectra of HY_{30} (black, top), TPS-HY_{30} (blue, middle) and $La(BH_4)_2(THF)_{2.5}$-TPS-HY_{30} (red, bottom), normalized to the zeolite framework signal at 1860 cm^{-1}.

$(THF)_n$-HY_{30}. DRIFTS revealed new bands at ≈2500 and 2200–2300 cm^{-1} (Figure S4) assigned to terminal and bridging $\nu_{B\text{-}H}$ from grafted borohydride species.[10a] Moreover, the normalized intensity of peaks associated with BAS diminished while the silanol signal retained similar intensity, suggesting that the La complex was selectively grafted at BAS and residual silanols are not accessible. ^{11}B direct-polarization (DP)MAS and multiple-quantum (MQ)MAS SS NMR spectra (Figures 2 and S6, respectively) of HY_{30}- and TPS-HY_{30}-supported catalysts showed one broad signal at 5 ppm assigned to BO_xH_y and two signals at −15 and −22 ppm assigned to BH_4^- groups in $La(BH_4)_x$ species.[8b,10a] BO_xH_y and BH_4^- species are present in a ≈2:1 ratio. We also tentatively assign the ^{11}B NMR signals at −22 and −15 ppm to silanol-grafted ≡SiO–$La(BH_4)_2$ and BAS-grafted ≡Si(≡Al)O–$La(BH_4)_2$ sites, respectively. The more shielded signal matches the chemical shift of the material obtained by grafting $La(BH_4)_3(THF)_3$ on silica.[10a] The −15 ppm signal is assigned as ≡Si(≡Al)O–$La(BH_4)_2$ because this peak is present in the aluminum-containing HY_{30}-grafted materials and not silica-grafted materials. In addition, its intensity increases relative to the ≡SiO–$La(BH_4)_2$ signal after selective capping of silanols, which increased the proportion of BAS-grafted sites.

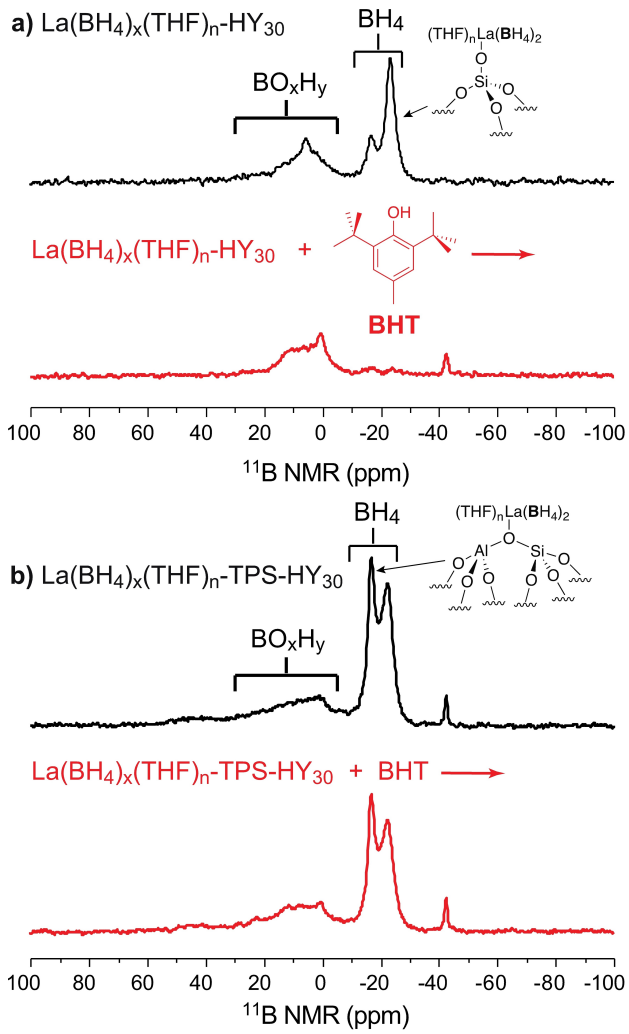

Figure 2. ^{11}B DPMAS NMR spectra of a) $La(BH_4)_x(THF)_n$-HY_{30} and b) $La(BH_4)_2(THF)_{2.5}$-TPS-HY_{30} before (black) and after (red) reaction with BHT.

In addition, elemental analysis (EA) revealed a ca. 3.2:1 ratio of B:La in the TPS-HY_{30}-supported catalyst (Table S2). Thus, NMR and EA data suggest that the B_2H_6 byproduct from borohydride protonolysis reacts with the zeolite. The final composition of the active site is assigned as $La(BH_4)_2(THF)_{2.5}$-TPS-HY_{30} from these data and the loss of one THF per two La after grafting revealed by quantitative solution-phase ^1H NMR (Figure S3).

The spatial and site selectivity of La grafting was further established by a poisoning spectrochemical analysis (see Supporting Information). Reaction of $La(BH_4)_x(THF)_n$-HY_{30} with 3,5-di-*t*-butyl-4-hydroxytoluene (BHT) resulted in almost complete disappearance of $[BH_4]^-$ signals in the ^{11}B SS NMR spectrum (Figure 2a). In contrast, an experiment involving $La(BH_4)_2(THF)_{2.5}$-TPS-HY_{30} under the same conditions gave a similar ^{11}B SS NMR spectrum to that of the TPS-decorated starting materials (Figure 2b). The ≈7.0× 9.3 Å estimated molecular dimensions of BHT impede its easy diffusion through the HY_{30} micropores. These experiments are wholly consistent with $La(BH_4)_3(THF)_3$ grafting primarily inside the micropores in the TPS-capped zeolite. In contrast, most of the lanthanum borohydride grafts on the external surface of uncapped HY_{30}, with a minority of active species grafted at BAS.

The $La(BH_4)_2(THF)_{2.5}$-TPS-HY_{30}-catalyzed reaction of benzene and HBpin at 120 °C gives PhBpin in substantially improved yield and turnovers (7.4±0.3 % and 62±3, respectively). The four-fold increase in PhBpin yield and six-fold increase in turnovers validates our silanol-capping approach, indicates that a larger fraction of BAS reacts with the La precursor after TPS capping and matches the ^{11}B NMR data. This result also affirms the hypothesis that ≡Si(≡Al)O–$La(BH_4)_2$-type sites lead to catalytically active benzene borylation.

A time-resolved study of the $La(BH_4)_2(THF)_{2.5}$-TPS-HY_{30}-catalyzed benzene borylation revealed a ≈6 h half-life for HBpin and a linear increase in turnovers over that time (Figure 3). The much longer half-life for HBpin during benzene borylation than during its TPS-HY_{30}-mediated decomposition (<2 h) indicates that this modified catalyst contains few accessible BAS to mediate the unwanted pathway. The rate of PhBpin formation has zero-order dependence in [HBpin]. Comparison of the slopes of turnovers vs time for borylation reactions of benzene and benzene-d_6 revealed a kinetic isotope effect (k_H/k_D=2.9), which is in the range of metalations of sp^2 hybridized C–H bonds via σ-bond metathesis steps.[3b]

Because the rate of HBpin decomposition depends on its concentration (Figure S7), reactions employing low [HBpin] could lead to increased yields and improved selectivity. This idea was tested through experiments in which HBpin was added in smaller portions (0.69 mol every 6 h) to a heated mixture of benzene and the $La(BH_4)_2(THF)_{2.5}$-TPS-HY_{30} catalyst (Figure 4). Addition of HBpin in 3 portions (totaling 2.1 mmol) gave full conversion of HBpin, 101 turnovers, and

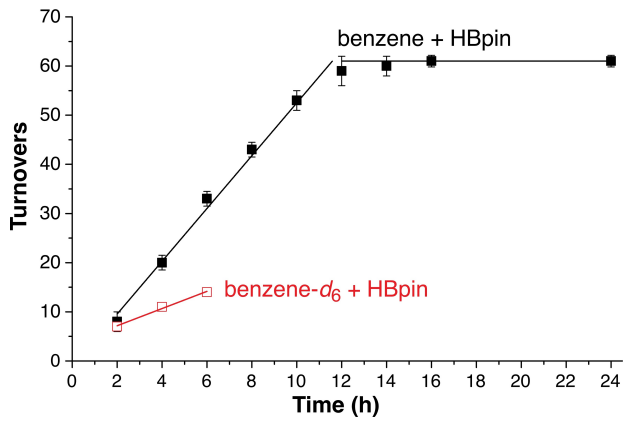

Figure 3. Benzene borylation, catalyzed by $La(BH_4)_2(THF)_{2.5}$-TPS-HY_{30}, showing zero-order concentration dependence for PhBpin production and a small, normal kinetic isotope effect for C–H/C–D bond activation.

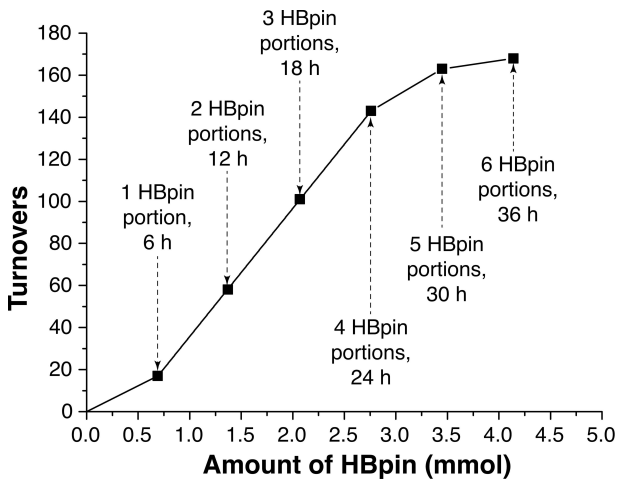

Figure 4. Portion-wise addition of HBpin (0.10 mL, 0.69 mmol every 6 h) in benzene borylation.

12 % yield of PhBpin after 18 h, which favorably compares to the 62 turnovers and 7.4 % yield from the experiment involving an addition of HBpin in a single portion. Clearly, the inequivalent [HBpin] dependences for benzene borylation and HBpin decomposition may be leveraged to access higher catalytic performance.

Addition of 2.8 mmol of HBpin in four portions gave 143 turnovers, corresponding to a linear increase in product over 24 h. Smaller increases, however, were observed in subsequent additions of HBpin. For example, addition of 4.1 mmol divided over six portions gave the maximum TON of 167. Separation of the catalytic material from the PhBpin product and HBpin decomposition product after addition of four portions of HBpin, washing the material with pentane and drying, and performing additional catalytic experiments provide approximately equivalent conversion as addition of HBpin *in situ*. Thus, under these conditions, the catalyst begins to deactivate for PhBpin production after ≈140 turnovers. We suspect that the side reactions which decompose HBpin are also related to catalyst deactivation, since these conditions that lead to greater selectivity also provide a higher absolute TON. Thus, improved yields and TON are likely achievable by avoiding HBpin decomposition, giving comparable performance to iridium catalysts (Table S3).

In conclusion, the identification of BAS both as detrimental, leading to HBpin decomposition, and as essential for creating the reactive lanthanum sites for benzene borylation enables future systematic and rational investigations to design catalysts with greater selectivity and efficiency. In this context, the porous and crystalline zeolite framework is particularly enticing, giving specific loadings of BAS which are either accessible or inaccessible based on the size and shape of the reactant. We are currently investigating these catalysts for such molecular sieving properties in reactive separations and to access enhanced selectivity. In addition, the behavior of C–H borylation versus HBpin decomposition at lower HBpin concentrations, suggested by the observed rate law, further implies improved conversions will develop by influencing concentrations of HBpin and reactant in microporous environment of the catalytic sites.

Acknowledgements

This research was supported by the U.S. Department of Energy (DOE), Office of Basic Energy Sciences, Division of Chemical Sciences, Geosciences, and Biosciences. The Ames Laboratory is operated for the U.S. DOE by Iowa State University under Contract No. DE-AC02-07CH11358. Open access funding provided by the Iowa State University Library.

Conflict of Interest

The authors declare no conflict of interest.

Data Availability Statement

The data that support the findings of this study are available in the Supporting Information of this article.

Keywords: Borylation · C–H Activation · Rare-Earth Elements · Supported Organometallic Catalysts · Zeolite

[1] a) A. K. Cook, S. D. Schimler, A. J. Matzger, M. S. Sanford, *Science* **2016**, *351*, 1421–1424; b) K. T. Smith, S. Berritt, M. González-Moreiras, S. Ahn, M. R. Smith, M.-H. Baik, D. J. Mindiola, *Science* **2016**, *351*, 1424–1427; c) M. R. Jones, C. D. Fast, N. D. Schley, *J. Am. Chem. Soc.* **2020**, *142*, 6488–6492; d) R.-L. Zhong, S. Sakaki, *J. Am. Chem. Soc.* **2020**, *142*, 16732–16747.

[2] a) J. F. Hartwig, *Acc. Chem. Res.* **2012**, *45*, 864–873; b) T. Ishiyama, J. Takagi, K. Ishida, N. Miyaura, N. R. Anastasi, J. F. Hartwig, *J. Am. Chem. Soc.* **2002**, *124*, 390–391; c) J.-Y. Cho, M. K. Tse, D. Holmes, R. E. Maleczka, M. R. Smith, *Science* **2002**, *295*, 305–308.

[3] a) P. L. Watson, G. W. Parshall, *Acc. Chem. Res.* **1985**, *18*, 51–56; b) M. E. Thompson, S. M. Baxter, A. R. Bulls, B. J. Burger, M. C. Nolan, B. D. Santarsiero, W. P. Schaefer, J. E. Bercaw, *J. Am. Chem. Soc.* **1987**, *109*, 203–219; c) G. M. Smith, M. Sabat, T. J. Marks, *J. Am. Chem. Soc.* **1987**, *109*, 1854–1856.
[4] a) J. Corker, F. Lefebvre, C. Lécuyer, V. Dufaud, F. Quignard, A. Choplin, J. Evans, J.-M. Basset, *Science* **1996**, *271*, 966–969; b) A. D. Sadow, T. D. Tilley, *Angew. Chem. Int. Ed.* **2003**, *42*, 803–805; *Angew. Chem.* **2003**, *115*, 827–829; c) A. D. Sadow, T. D. Tilley, *J. Am. Chem. Soc.* **2005**, *127*, 643–656.
[5] R. Waterman, *Organometallics* **2013**, *32*, 7249–7263.
[6] D. H. Motry, M. R. Smith, *J. Am. Chem. Soc.* **1995**, *117*, 6615–6616.
[7] C. Xue, Y. Luo, H. Teng, Y. Ma, M. Nishiura, Z. Hou, *ACS Catal.* **2018**, *8*, 5017–5022.
[8] a) S. Patnaik, A. D. Sadow, *Angew. Chem. Int. Ed.* **2019**, *58*, 2505–2509; *Angew. Chem.* **2019**, *131*, 2527–2531; b) Z. Wang, S. Patnaik, N. Eedugurala, J. S. Manzano, I. I. Slowing, T. Kobayashi, A. D. Sadow, M. Pruski, *J. Am. Chem. Soc.* **2020**, *142*, 2935–2947.
[9] a) M. Visseaux, F. Bonnet, *Coord. Chem. Rev.* **2011**, *255*, 374–420; b) D. Robert, M. Kondracka, J. Okuda, *Dalton Trans.* **2008**, 2667–2669.
[10] a) N. Ajellal, G. Durieux, L. Delevoye, G. Tricot, C. Dujardin, C. M. Thomas, R. M. Gauvin, *Chem. Commun.* **2010**, *46*, 1032–1034; b) I. D. Rosal, M. J.-L. Tschan, R. M. Gauvin, L. Maron, C. M. Thomas, *Polym. Chem.* **2012**, *3*, 1730–1739.
[11] a) X. Zhang, Z. Huang, M. Ferrandon, D. Yang, L. Robison, P. Li, T. C. Wang, M. Delferro, O. K. Farha, *Nat. Catal.* **2018**, *1*, 356–362; b) X. Feng, Y. Song, Z. Li, M. Kaufmann, Y. Pi, J. S. Chen, Z. Xu, Z. Li, C. Wang, W. Lin, *J. Am. Chem. Soc.* **2019**, *141*, 11196–11203; c) Z. H. Syed, Z. Chen, K. B. Idrees, T. A. Goetjen, E. C. Wegener, X. Zhang, K. W. Chapman, D. M. Kaphan, M. Delferro, O. K. Farha, *Organometallics* **2020**, *39*, 1123–1133; d) K. Manna, T. Zhang, W. Lin, *J. Am. Chem. Soc.* **2014**, *136*, 6566–6569; e) K. Manna, P. Ji, Z. Lin, F. X. Greene, A. Urban, N. C. Thacker, W. Lin, *Nat. Commun.* **2016**, *7*, 12610; f) K. Manna, T. Zhang, F. X. Greene, W. Lin, *J. Am. Chem. Soc.* **2015**, *137*, 2665–2673; g) R. Newar, W. Begum, N. Antil, S. Shukla, A. Kumar, N. Akhtar, Balendra, K. Manna, *Inorg. Chem.* **2020**, *59*, 10473–10481.
[12] a) M. Waki, Y. Maegawa, K. Hara, Y. Goto, S. Shirai, Y. Yamada, N. Mizoshita, T. Tani, W.-J. Chun, S. Muratsugu, M. Tada, A. Fukuoka, S. Inagaki, *J. Am. Chem. Soc.* **2014**, *136*, 4003–4011; b) W. R. Grüning, G. Siddiqi, O. V. Safonova, C. Copéret, *Adv. Synth. Catal.* **2014**, *356*, 673–679; c) Y. Maegawa, S. Inagaki, *Dalton Trans.* **2015**, *44*, 13007–13016.
[13] a) Y. Li, L. Li, J. Yu, *Chem* **2017**, *3*, 928–949; b) S. Grundner, M. A. C. Markovits, G. Li, M. Tromp, E. A. Pidko, E. J. M. Hensen, A. Jentys, M. Sanchez-Sanchez, J. A. Lercher, *Nat. Commun.* **2015**, *6*, 7546; c) I. Ogino, B. C. Gates, *J. Am. Chem. Soc.* **2008**, *130*, 13338–13346.
[14] I. C. Medeiros-Costa, E. Dib, N. Nesterenko, J.-P. Dath, J.-P. Gilson, S. Mintova, *Chem. Soc. Rev.* **2021**, *50*, 11156–11179.
[15] O. Cairon, T. Chevreau, J.-C. Lavalley, *J. Chem. Soc. Faraday Trans.* **1998**, *94*, 3039–3047.
[16] S. Prodinger, M. A. Derewinski, A. Vjunov, S. D. Burton, I. Arslan, J. A. Lercher, *J. Am. Chem. Soc.* **2016**, *138*, 4408–4415.
[17] E. Brendler, T. Heine, W. Seichter, J. Wagler, R. Witter, *Z. Anorg. Allg. Chem.* **2012**, *638*, 935–944.

Manuscript received: December 20, 2021
Accepted manuscript online: February 1, 2022
Version of record online: February 18, 2022